

## Damped resonant steady-state sloshing in an upright circular tank\*

*I. A. Raynovskyy*<sup>1</sup>, *A. N. Timokha*<sup>1,2</sup>

<sup>1</sup> *Institute of Mathematics of NAS of Ukraine, Kyiv;*  
*ihor.raynovskyy@gmail.com*

<sup>2</sup> *Centre of Excellence AMOS, Norwegian University of Science and Technology, Trondheim, Norway;* *atimokha@gmail.com.*

The nonlinear Narimanov–Moiseev-type modal system with linear damping terms is employed to study the damped steady-state resonant sloshing in an upright circular tank. Estimating the damping coefficients (ratios) by using Miles' formula shows that the damping may matter for laboratory tanks. An asymptotic steady-state solution of the modal system is derived for a prescribed cyclic tank motion with four (sway/surge/pitch/roll) degrees of freedom; the forcing frequency is close to the lowest natural sloshing frequency. The steady-state response curves by the two lowest-order natural sloshing mode amplitudes are examined versus the semi-axes ratio of the artificial elliptic orbit.

Використовуючи нелінійну модальну систему Наріманова–Мойсеева із лінійними коефіцієнтами демпфування, вивчаються усталені демпфовані резонансні хлюпання рідини у циліндричному баку. Оцінка коефіцієнтів демпфування за допомогою формули Майлза показує, що демпфування може мати значення для лабораторних посудин. Знайдено асимптотичний усталений розв'язок модальної системи для заданого руху циліндричної посудини із чотирма (sway/surge/pitch/roll) ступенями вільності; частота збурення є близькою до найнижчої власної частоти коливань рідини. Розглянуто залежність амплітудно-частотних характеристик, що пов'язуються із амплітудами двох нижчих власних форм коливання рідини від співвідношення півосей еліптичної орбіти.

---

\*The work is partly supported by the Grant № 0117U004077. The second author acknowledges the financial support of the Centre of Autonomous Marine Operations and Systems (AMOS) whose main sponsor is the Norwegian Research Council (Project number 223254-AMOS).

## 1 Introduction

Steady-state resonant sloshing in an upright circular cylindrical tank due to a harmonic longitudinal excitation with the forcing frequency close to the lowest natural frequency has been studied by many authors, theoretically and experimentally, starting from the 60's. Most recent reviews can be found in [10, 12, 18]. In the theoretical studies, the linear liquid damping caused by boundary layer and bulk viscosity effects (see derivations of the associated logarithmic decrements in [5, 14]) was normally neglected. The latter was supported by experiments with industrial containers whose geometric dimensions count in metres but [2, 7, 9, 16, 17, 19] showed that the damping may matter for certain small laboratory tanks incl. bioreactors. Reasons are an increasing viscosity of the bioliquids and a growing effect of the dynamic contact angle.

Bioreactors normally perform orbital periodic motions with the forcing frequency close to the lowest natural sloshing frequency. Those tank excitations were considered in [3, 15] within the framework of an inviscid potential flow model. The undamped steady-state sloshing regimes were classified for an elliptic horizontal forcing by using an infinite-dimensional Narimanov–Moiseev-type nonlinear modal system, which couples the generalised coordinates of the natural sloshing modes. The present paper includes the linear damping effect into the steady-state analysis of [3].

In § 2, we introduce the Narimanov–Moiseev-type modal system equipped with linear damping terms whose (damping) coefficients are associated with boundary layer and bulk viscosity effects onto the corresponding natural sloshing modes. A theoretical estimate of the damping coefficients is given in § 3 following Miles' analysis [14]. Numerical analysis with the tap water shows that these coefficients are negligibly small for industrial containers but, indeed, the linear damping may matter for smaller tanks.

An analytical asymptotic periodic solution of the Narimanov–Moiseev-type modal system is constructed in § 4. The solution describes resonant steady-state wave regimes when tank performs an orbital motion with four degrees (sway/surge/roll/pitch) of freedom. These regimes are asymptotically equivalent to those occurring due to an elliptic horizontal tank excitation as has been postulated in [3]. The present study focuses on the *damped* steady-state wave regimes and their stability versus the ellipse semi-axes ratio  $0 \leq \delta \leq 1$  whose limit values 0 and 1 correspond to longitudinal and rotary prescribed tank motions, respectively. Clas-

sification of these regimes requires analysing a secular system of four nonlinear algebraic equations coupling the lowest-order amplitudes  $a, \bar{b}$  and  $\bar{a}, b$ , which correspond to sin and cos components of the two lowest natural sloshing modes. The system has an analytical solution for the undamped case [3, 15] but it does not in the studied case. A reason is appearance of the damping-caused phase-lags. The secular system is then re-written in terms of the integral amplitudes  $A = \sqrt{A^2 + \bar{a}^2}$  and  $B = \sqrt{\bar{b}^2 + b^2}$ . In § 5, the steady-state results are interpreted in terms of response curves drawn in the  $(\sigma/\sigma_1, A, B)$  space where  $\sigma$  is the forcing frequency and  $\sigma_1$  is the lowest natural sloshing frequency.

## 2 Statement of the problem

An incompressible inviscid liquid with an irrotational flow is considered partly filling an upright circular rigid tank of the radius  $r_0$ . The tank performs a small-magnitude prescribed periodic sway/surge/roll/pitch motion, which is described by the  $r_0$ -scaled generalised coordinates  $\eta_1(t)$ ,  $\eta_2(t)$  and  $\eta_4(t)$ ,  $\eta_5(t)$ , respectively, as shown in figure 1. The yaw type tank motions cannot excite sloshing within the framework of the inviscid flow model but the heave (vertical) oscillations are not considered in the present paper (see a review on the parametrically-excited sloshing in [6]). The problem is studied in the nondimensional statement, which is based on the characteristic size  $r_0$  and time  $1/\sigma$ , where  $\sigma$  is the forcing frequency. A small parameter  $0 < \epsilon \ll 1$  is introduced. It is associated with the nondimensional periodic forcing magnitude, i.e.  $\eta_i(t) = O(\epsilon)$ ,  $i = 1, 2, 4, 5$ .

Figure 1 illustrates the time-dependent liquid domain  $Q(t)$  with the free surface  $\Sigma(t)$  (governed by the single-valued function  $z = \zeta(r, \theta, t)$ ) and the wetted tank surface  $S(t)$ ;  $\Phi(r, \theta, z, t)$  is the velocity potential. The unknowns,  $\zeta$  and  $\Phi$ , are defined in the tank-fixed coordinate system. They can be found from either the corresponding free-surface problem or its equivalent variational formulation.

Using the Fourier-type representations of  $\zeta$  and  $\Phi$  and the aforementioned variational formulation makes it possible to derive [3] an approximate system of ordinary differential equations (nonlinear modal equations) with respect to the time-dependent coefficients in these representations. The coefficients are interpreted as *generalised coordinates and velocities*, respectively. The Fourier basis consists of the natural sloshing

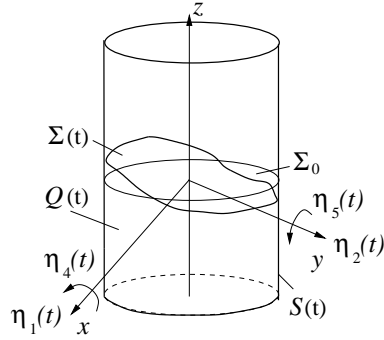


**Figure 1.** The liquid domain  $Q(t)$  is confined by the free surface  $\Sigma(t)$  and the wetted tank surface  $S(t)$ . Sloshing is considered in the tank-fixed coordinate system  $Oxyz$  whose coordinate plane  $Oxy$  coincides with the mean (hydrostatic) free surface  $\Sigma_0$ ;  $Oz$  is the symmetry axis. Small-magnitude periodic tank excitations are governed by generalised coordinates  $\eta_1(t)$  (surge),  $\eta_4(t)$  (roll),  $\eta_2(t)$  (sway), and  $\eta_5(t)$  (pitch).

(eigen) modes  $\varphi_{Mi}$  following from the spectral boundary problem

$$\nabla^2 \varphi = 0 \text{ in } Q_0, \quad \frac{\partial \varphi}{\partial n} = 0 \text{ on } S_0, \quad \frac{\partial \varphi}{\partial n} = \kappa \varphi \text{ on } \Sigma_0, \quad \int_{\Sigma_0} \varphi \, dS = 0, \quad (1)$$

where  $Q_0$  is the mean (hydrostatic) liquid domain confined by the mean free surface  $\Sigma_0$  and the wetted tank surface  $S_0$  (figure 1). The problem (1) has the analytical solution [4, 10]:

$$\varphi_{Mi}(r, z, \theta) = \mathcal{R}_{Mi}(r) \mathcal{Z}_{Mi}(z) \frac{\cos}{\sin}(M\theta), \quad M = 0, \dots; \quad i = 1, \dots, \quad (2a)$$

$$\mathcal{R}_{Mi}(r) = \alpha_{Mi} J_M(k_{Mi}r), \quad \mathcal{Z}_{Mi}(z) = \frac{\cosh(k_{Mi}(z+h))}{\cosh(k_{Mi}h)}, \quad (2b)$$

where  $J_M(\cdot)$  is the Bessel functions of the first kind, the radial wave numbers  $k_{Mi}$  are determined by the transcendental equation  $\mathcal{R}'_{Mi}(1) = 0$  (equivalent to  $J'_{Mi}(k_{Mi}) = 0$ ) and the normalising multipliers  $\alpha_{Mi}$  follow from the orthogonality condition

$$\lambda_{(Mi)(Mj)} = \int_{r_1}^1 r \mathcal{R}_{Mi}(r) \mathcal{R}_{Mj}(r) \, dr = \delta_{ij}, \quad i, j = 1, \dots, \quad (3)$$

where  $\delta_{ij}$  is the Kronecker delta. The nondimensional eigenvalues  $\kappa_{Mi}$  and the dimensional natural sloshing frequencies  $\sigma_{Mi}$  are computed by

the formulas

$$\kappa_{Mi} = k_{Mi} \tanh(k_{Mi}h) \quad (J'_{Mi}(k_{Mi}) = 0) \quad \text{and} \quad \sigma_{Mi}^2 = \kappa_{Mi} g / r_0, \quad (4)$$

where  $g = 9.81 \text{ [m/s}^2\text{]}$  is the dimensional gravity acceleration.

Because we consider small-amplitude angular tank motions, the modal representations require to know the linearised Stokes-Joukowski potentials  $\Omega_{0i}(r, z, \theta)$ ,  $i = 1, 2, 3$  (see definition and analytical details in [3, 12]). The potentials are harmonic functions satisfying the Neumann boundary conditions

$$\frac{\partial \Omega_{01}}{\partial n} = -(zn_r - rn_z) \sin \theta, \quad \frac{\partial \Omega_{02}}{\partial n} = (zn_r - rn_z) \cos \theta, \quad \frac{\partial \Omega_{03}}{\partial n} = 0 \quad (5)$$

on  $\Sigma_0$  and  $S_0$ , where  $n_r$  and  $n_z$  are the outer normal components in the  $r$ - and  $z$ - directions, respectively. The Stokes-Joukowski potentials have the analytical form  $\Omega_{01} = -F(r, z) \sin \theta$ ,  $\Omega_{02} = F(r, z) \cos \theta$ ,  $\Omega_{03} = 0$ , where

$$F(r, z) = rz - \sum_{n=1}^{\infty} \frac{2P_n}{k_{1n}} \mathcal{R}_{1n}(r) \frac{\sinh(k_{1n}(z + \frac{1}{2}h))}{\cosh(\frac{1}{2}k_{1n}h)}; \quad P_n = \int_{r_1}^1 r^2 \mathcal{R}_{1n}(r) dr. \quad (6)$$

Based on (2a) and (6), the Fourier representation takes the form [3]

$$\zeta(r, \theta, t) = \sum_{M,i}^{I_\theta, I_r} \mathcal{R}_{Mi}(r) \cos(M\theta) p_{Mi}(t) + \sum_{m,i}^{I_\theta, I_r} \mathcal{R}_{mi}(r) \sin(m\theta) r_{mi}(t), \quad (7a)$$

$$\begin{aligned} \Phi(r, \theta, z, t) = & \dot{\eta}_1(t) r \cos \theta + \dot{\eta}_2(t) r \sin \theta + F(r, z) [-\dot{\eta}_4(t) \sin \theta + \dot{\eta}_5(t) \cos \theta] \\ & + \sum_{M,i}^{I_\theta, I_r} \mathcal{R}_{Mi}(r) \mathcal{Z}_{Mi}(z) \cos(M\theta) P_{Mi}(t) \\ & + \sum_{m,i}^{I_\theta, I_r} \mathcal{R}_{mi}(r) \mathcal{Z}_{mi}(z) \sin(m\theta) R_{mi}(t), \quad (7b) \end{aligned}$$

$I_\theta, I_r \rightarrow \infty$ , where  $p_{Mi}(t)$  and  $r_{mi}(t)$  are the free-surface generalised coordinates but  $P_{Mi}(t)$  and  $R_{mi}(t)$  are the generalised velocities. *Furthermore*, all capital summation letters imply changing from zero to  $I_\theta$  but the lower case indices mean changing from one to either  $I_\theta$  or  $I_r$ .

In [3], using the Bateman–Luke variational formalism, the modal representation (7), the Narimanov-Moiseev asymptotic relations

$$\begin{aligned} p_{11} \sim r_{11} = O(\epsilon^{1/3}), \quad p_{0j} \sim p_{2j} \sim r_{2j} = O(\epsilon^{2/3}), \\ r_{1(j+1)} \sim p_{1(j+1)} \sim p_{3j} \sim r_{3j} = O(\epsilon), \quad j = 1, 2, \dots, I_r; \quad I_r \rightarrow \infty \end{aligned} \quad (8)$$

and the Moiseev resonant detuning (measuring how close is the forcing frequency to the lowest natural sloshing frequency)

$$\bar{\sigma}_{11}^2 - 1 = O(\epsilon^{2/3}), \quad \bar{\sigma}_{Mi} = \sigma_{Mi}/\sigma \quad (9)$$

(see an extensive discussion on what (8) and (9) mean for axisymmetric tanks in [11]), the following weakly-nonlinear system of ordinary differential (modal) equations with respect to the generalised coordinates were derived

$$\begin{aligned} \ddot{p}_{11} + \boxed{2\xi_{11}\bar{\sigma}_{11}\dot{p}_{11}} + \bar{\sigma}_{11}^2 p_{11} + d_1 p_{11} (\ddot{p}_{11} p_{11} + \ddot{r}_{11} r_{11} + \dot{p}_{11}^2 + \dot{r}_{11}^2) \\ + d_2 [r_{11}(\ddot{p}_{11} r_{11} - \ddot{r}_{11} p_{11}) + 2\dot{r}_{11}(\dot{p}_{11} r_{11} - \dot{r}_{11} p_{11})] \\ + \sum_{j=1}^{I_r} \left[ d_3^{(j)} (\ddot{p}_{11} p_{2j} + \ddot{r}_{11} r_{2j} + \dot{p}_{11} \dot{p}_{2j} + \dot{r}_{11} \dot{r}_{2j}) + d_4^{(j)} (\ddot{p}_{2j} p_{11} + \ddot{r}_{2j} r_{11}) \right. \\ \left. + d_5^{(j)} (\ddot{p}_{11} p_{0j} + \dot{p}_{11} \dot{p}_{0j}) + d_6^{(j)} \ddot{p}_{0j} p_{11} \right] = -(\ddot{\eta}_1 - g\eta_5 - S_1 \ddot{\eta}_5) \kappa_{11} P_1, \end{aligned} \quad (10a)$$

$$\begin{aligned} \ddot{r}_{11} + \boxed{2\xi_{11}\bar{\sigma}_{11}\dot{r}_{11}} + \bar{\sigma}_{11}^2 r_{11} + d_1 r_{11} (\ddot{p}_{11} p_{11} + \ddot{r}_{11} r_{11} + \dot{p}_{11}^2 + \dot{r}_{11}^2) \\ + d_2 [p_{11}(\ddot{r}_{11} p_{11} - \ddot{p}_{11} r_{11}) + 2\dot{p}_{11}(\dot{r}_{11} p_{11} - \dot{p}_{11} r_{11})] \\ + \sum_{j=1}^{I_r} \left[ d_3^{(j)} (\ddot{p}_{11} r_{2j} - \ddot{r}_{11} p_{2j} + \dot{p}_{11} \dot{r}_{2j} - \dot{p}_{2j} \dot{r}_{11}) + d_4^{(j)} (\ddot{r}_{2j} p_{11} - \ddot{p}_{2j} r_{11}) \right. \\ \left. + d_5^{(j)} (\ddot{r}_{11} p_{0j} + \dot{r}_{11} \dot{p}_{0j}) + d_6^{(j)} \ddot{p}_{0j} r_{11} \right] = -(\ddot{\eta}_2 + g\eta_4 + S_1 \ddot{\eta}_4) \kappa_{11} P_1; \end{aligned} \quad (10b)$$

$$\ddot{p}_{2k} + \boxed{2\xi_{2k}\bar{\sigma}_{2k}\dot{p}_{2k}} + \bar{\sigma}_{2k}^2 p_{2k} + d_{7,k}(\dot{p}_{11}^2 - \dot{r}_{11}^2) + d_{9,k}(\ddot{p}_{11} p_{11} - \ddot{r}_{11} r_{11}) = 0, \quad (11a)$$

$$\ddot{r}_{2k} + \boxed{2\xi_{2k}\bar{\sigma}_{2k}\dot{r}_{2k}} + \bar{\sigma}_{2k}^2 r_{2k} + 2d_{7,k}\dot{p}_{11}\dot{r}_{11} + d_{9,k}(\ddot{p}_{11} r_{11} + \ddot{r}_{11} p_{11}) = 0, \quad (11b)$$

$$\ddot{p}_{0k} + \boxed{2\xi_{0k}\bar{\sigma}_{0k}\dot{p}_{0k}} + \bar{\sigma}_{0k}^2 p_{0k} + d_{8,k}(\dot{p}_{11}^2 + \dot{r}_{11}^2) + d_{10,k}(\ddot{p}_{11} p_{11} + \ddot{r}_{11} r_{11}) = 0; \quad (11c)$$

$$\begin{aligned}
& \ddot{p}_{3k} + \boxed{2\xi_{3k}\bar{\sigma}_{3k}\dot{p}_{3k}} + \bar{\sigma}_{3k}^2 p_{3k} + d_{11,k} [\dot{p}_{11}(p_{11}^2 - r_{11}^2) - 2p_{11}r_{11}\dot{r}_{11}] \\
& + d_{12,k} [p_{11}(\dot{p}_{11}^2 - \dot{r}_{11}^2) - 2r_{11}\dot{p}_{11}\dot{r}_{11}] + \sum_{j=1}^{I_r} \left[ d_{13,k}^{(j)} (\ddot{p}_{11}p_{2j} - \ddot{r}_{11}r_{2j}) \right. \\
& \left. + d_{14,k}^{(j)} (\ddot{p}_{2j}p_{11} - \ddot{r}_{2j}r_{11}) + d_{15,k}^{(j)} (\dot{p}_{2j}\dot{p}_{11} - \dot{r}_{2j}\dot{r}_{11}) \right] = 0, \quad (12a)
\end{aligned}$$

$$\begin{aligned}
& \ddot{r}_{3k} + \boxed{2\xi_{3k}\bar{\sigma}_{3k}\dot{r}_{3k}} + \bar{\sigma}_{3k}^2 r_{3k} + d_{11,k} [\ddot{r}_{11}(p_{11}^2 - r_{11}^2) + 2p_{11}r_{11}\ddot{p}_{11}] \\
& + d_{12,k} [r_{11}(\dot{p}_{11}^2 - \dot{r}_{11}^2) + 2p_{11}\dot{p}_{11}\dot{r}_{11}] + \sum_{j=1}^{I_r} \left[ d_{13,k}^{(j)} (\ddot{p}_{11}r_{2j} + \ddot{r}_{11}p_{2j}) \right. \\
& \left. + d_{14,k}^{(j)} (\ddot{p}_{2j}r_{11} + \ddot{r}_{2j}p_{11}) + d_{15,k}^{(j)} (\dot{p}_{2j}\dot{r}_{11} + \dot{r}_{2j}\dot{p}_{11}) \right] = 0, \quad k = 1, \dots, I_r; \quad (12b)
\end{aligned}$$

$$\begin{aligned}
& \ddot{p}_{1n} + \boxed{2\xi_{1n}\bar{\sigma}_{1n}\dot{p}_{1n}} + \bar{\sigma}_{1n}^2 p_{1n} + d_{16,n} (\ddot{p}_{11}p_{11}^2 + r_{11}p_{11}\ddot{r}_{11}) \\
& + d_{17,n} (\ddot{p}_{11}r_{11}^2 - r_{11}p_{11}\ddot{r}_{11}) + d_{18,n} p_{11} (\dot{p}_{11}^2 + \dot{r}_{11}^2) + d_{19,n} (r_{11}\dot{p}_{11}\dot{r}_{11} - p_{11}\dot{r}_{11}^2) \\
& + \sum_{j=1}^{I_r} \left[ d_{20,n}^{(j)} (\ddot{p}_{11}p_{2j} + \ddot{r}_{11}r_{2j}) + d_{21,n}^{(j)} (p_{11}\ddot{p}_{2j} + r_{11}\ddot{r}_{2j}) \right. \\
& \left. + d_{22,n}^{(j)} (\dot{p}_{11}\dot{p}_{2j} + \dot{r}_{11}\dot{r}_{2j}) + d_{23,n}^{(j)} \ddot{p}_{11}p_{0j} + d_{24,n}^{(j)} p_{11}\ddot{p}_{0j} + d_{25,n}^{(j)} \dot{p}_{11}\dot{p}_{0j} \right] \\
& = -(\ddot{\eta}_1 - g\eta_5 - S_n\ddot{\eta}_5)\kappa_{1n}P_n, \quad (13a)
\end{aligned}$$

$$\begin{aligned}
& \ddot{r}_{1n} + \boxed{2\xi_{1n}\bar{\sigma}_{1n}\dot{r}_{1n}} + \bar{\sigma}_{1n}^2 r_{1n} + d_{16,n} (\ddot{r}_{11}r_{11}^2 + r_{11}p_{11}\ddot{p}_{11}) \\
& + d_{17,n} (\ddot{r}_{11}p_{11}^2 - r_{11}p_{11}\ddot{p}_{11}) + d_{18,n} r_{11} (\dot{p}_{11}^2 + \dot{r}_{11}^2) + d_{19,n} (p_{11}\dot{p}_{11}\dot{r}_{11} - r_{11}\dot{p}_{11}^2) \\
& + \sum_{j=1}^{I_r} \left[ d_{20,n}^{(j)} (\ddot{p}_{11}r_{2j} - \ddot{r}_{11}p_{2j}) + d_{21,n}^{(j)} (p_{11}\ddot{r}_{2j} - r_{11}\ddot{p}_{2j}) + d_{22,n}^{(j)} (\dot{p}_{11}\dot{r}_{2j} - \dot{r}_{11}\dot{p}_{2j}) \right. \\
& \left. + d_{23,n}^{(j)} \ddot{r}_{11}p_{0j} + d_{24,n}^{(j)} r_{11}\ddot{p}_{0j} + d_{25,n}^{(j)} \dot{r}_{11}\dot{p}_{0j} \right] \\
& = -(\ddot{\eta}_2 + g\eta_4 + S_n\ddot{\eta}_4)\kappa_{1n}P_n, \quad n = 2, \dots, I_r. \quad (13b)
\end{aligned}$$

The hydrodynamic coefficients are functions of the nondimensional liquid depth  $h/r_0$ . The system is equipped with the linear damping (framed)

terms, in which the damping coefficients are associated with the logarithmic decrements of the corresponding natural sloshing modes. By definition, the modal system (10)–(13) includes all up to the  $O(\epsilon)$ -order terms as  $I_r \rightarrow \infty$ ;  $r_{kl} \sim p_{kl} = o(\epsilon)$ ,  $k \geq 4$  are neglected. The system needs either initial or periodicity condition. The latter leads to the resonant steady-state wave regimes (solutions). The system (10)–(13) without damping terms (undamped sloshing) was extensively validated in [3] by comparisons with experiments for longitudinal resonant excitations.

### 3 Linear damping coefficients

When using (10)–(13) implicitly assumes the following conditions [3]:

- The nondimensional generalised coordinates  $\eta_i(t)$ ,  $i = 1, 2, 4, 5$ , are the given  $2\pi$ -periodic functions,

$$\eta_i(t) = \eta_{ia}^{(0)} + \sum_{k=1}^{\infty} \left[ \eta_{ia}^{(k)} \cos(kt) + \mu_{ia}^{(k)} \sin(kt) \right], \quad \eta_{ia}^{(k)} \sim \mu_{ia}^{(k)} = O(\epsilon), \quad (14)$$

where the lowest-order harmonic component is not zero, i.e.

$$\sum_{i=1,2,4,5} |\eta_{ia}^{(1)}| + |\mu_{ia}^{(1)}| \neq 0. \quad (15)$$

- The Moiseev detuning condition (9) is satisfied.
- There are no resonance amplifications of higher-order generalised coordinates  $p_{mj}, r_{mj}$ ,  $m, j \neq 1$ ,

$$\begin{aligned} m - \bar{\sigma}_{1k} &\geq O(1), \quad \bar{\sigma}_{mi} = \sigma_{mi}/\sigma, \quad m, k \geq 2; \\ \bar{\sigma}_{0i}^2 - 4 &\sim \bar{\sigma}_{2i}^2 - 4 \sim \bar{\sigma}_{3i}^2 - 9 \sim \bar{\sigma}_{1(i+1)}^2 - 9 \geq O(1), \quad i \geq 1. \end{aligned} \quad (16)$$

The second row of (16) means that there are no secondary resonances [3].

- Because (10)–(13) neglects the  $o(\epsilon)$ -order terms, the linear damping terms matter, if and only if,

$$\xi_{11} = O(\epsilon^{2/3}), \quad \xi_{2i} \sim \xi_{0i} = O(\epsilon^{1/3}), \quad \xi_{3i} \sim \xi_{1n} = O(1), \quad (17)$$

$i \geq 1, n \geq 2$  in the corresponding differential equations.

The damping ratios  $\xi_{Mi}$  were theoretically and experimentally estimated by many authors starting from the 50's [4, 14]. For low-viscous liquids, the theoretical estimates can be asymptotically expressed in terms of the *Galilei number* [1],  $\text{Ga}$  (regarded as a ratio between gravity and viscous forces),

$$\delta = \text{Ga}^{-1/4} = \sqrt{\nu/(g^{1/2}r_0^{3/2})} \ll 1, \quad (18)$$

where  $\nu$  is the kinematic viscosity. The lowest-order asymptotic contribution,  $\xi_{Mi}^{surf} = O(\delta)$ , is associated with the laminar boundary layer effect on the wetted tank surface;  $\xi_{Mi}^{surf}$  can be rather accurately approximated by using the Keulegan analytical technique [8]. The second-order asymptotic contribution,  $\xi_{Mi}^{bulk} = O(\delta^2)$ , is due to the bulk viscosity. According to [13, 14], a good agreement with experiments requires to account for both the contributions, i.e.

$$\xi_{Mi} = \xi_{Mi}^{surf} + \xi_{Mi}^{bulk}. \quad (19)$$

Miles [14] have found an analytical expression for (19). Using an alternative analytical scheme, we re-derived Miles' approximation as

$$\xi_{Mi}^{surf} = \delta \frac{\mu_{Mi}^{(1)} + \frac{1}{2}\mathcal{R}_{Mi}^2(1)(\mu_{Mi}^{(2)} + \mu_{Mi}^{(3)})}{2\sqrt{2}\kappa_{Mi}^{5/4}\mu_{Mi}^{(0)}}, \quad (20a)$$

$$\xi_{Mi}^{bulk} = \delta^2 \left[ \frac{2k_{Mi}^2}{\kappa_{Mi}^{1/2}} - \frac{\mathcal{R}_{Mi}^2(1)\mu_{Mi}^{(2)}}{2\kappa_{Mi}^{3/2}\mu_{Mi}^{(0)}} \right], \quad (20b)$$

where

$$\begin{aligned} \mu_{Mi}^{(0)} &= \int_0^1 r\mathcal{R}_{Mi}^2(r)dr, \quad \mu_{Mi}^{(1)} = \int_0^1 r\mathcal{R}_{Mi}'^2(r)dr + M^2 \int_0^1 \frac{\mathcal{R}_{Mi}^2(r)}{r}dr, \\ \mu_{Mi}^{(2)} &= M^2 \left( \frac{\tanh(k_{Mi}h)}{k_{Mi}} + \frac{h}{\cosh^2(k_{Mi}h)} \right), \\ \mu_{Mi}^{(3)} &= k_{Mi}^2 \left( \frac{\tanh(k_{Mi}h)}{k_{Mi}} - \frac{h}{\cosh^2(k_{Mi}h)} \right). \end{aligned} \quad (21)$$

The Galileo number  $\text{Ga} = gr_0^3/\nu^2$  is a function of the kinematic viscosity, the container radius  $r_0$  and  $g$ . Along with the Bond number  $\text{Bo} = \rho gr_0^2/T_s$  ( $\rho$  is the liquid density and the  $T_s$  is the surface tension),

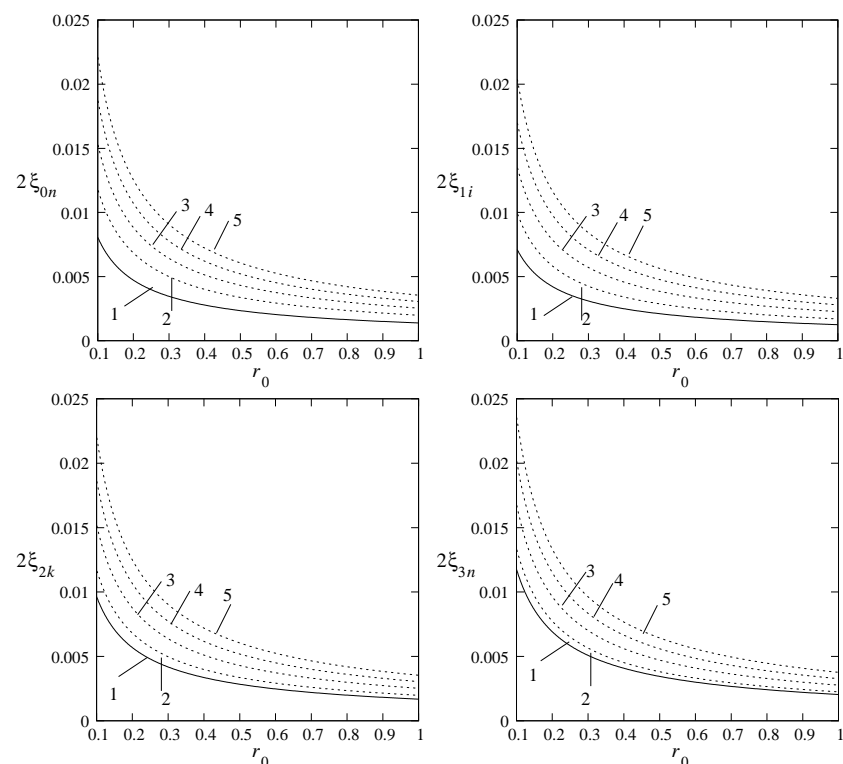


**Figure 2.** The theoretical damping rates  $2\xi_{Mi}$  by (19)–(21) for  $M = 0, 1, 2, 3$ . The tap water with  $\nu = 10^{-6}$  [m<sup>2</sup>/s] and  $g = 9.81$  [m/s<sup>2</sup>]. The second index is used to mark the curves.

the Galileo number is well-known in the microgravity hydromechanics [1].  $Bo$  and  $Ga$  are regarded as ratios between gravitational (mass forces) and surface/viscous forces, respectively. When  $100 \lesssim Bo$ , the surface tension effect can be neglected. For the tap liquid at the Earth conditions with  $\rho = 10^3$  [kg/m<sup>3</sup>] and  $T_s = 0.073$  [N/m], this inequality leads to  $0.05$  [m]  $\lesssim r_0$ , which is required in our study because the modal system (10)–(13) does not account for the surface tension.

Figure 2 demonstrates the damping rates *versus*  $r_0$  for the tap water. In view of the asymptotic relations (17), one can expect that the linear damping is negligible small for the industrial containers, whose the

nondimensional forcing amplitude  $\approx 0.001$  looks practically impossible. For small-size laboratory containers (e.g., bioreactors),  $2\xi_{11}$  may however satisfy (17). This is especially due to a higher viscosity of bioliquids as well as the dynamic contact angle effect [7, 8] and the surface/liquid contamination [5], which increase the amount dissipation.

#### 4 Steady-state resonant solution

Following [3], we construct an asymptotic periodic solution of (10)–(13) in terms of  $\epsilon^{1/3} \ll 1$ , which is associated with the primary excited generalised coordinates  $p_{11}(t)$  and  $r_{11}(t)$ . The right-hand sides of (10) take the form

$$\begin{aligned} \sigma^2 P_1 \kappa_{11} \sum_{k=1}^{\infty} & \left[ (k\eta_{1a}^{(k)} - (kS_1 - g/\sigma^2)\eta_{5a}^{(k)}) \cos(kt) \right. \\ & \left. + (k\mu_{1a}^{(k)} - (kS_1 - g/\sigma^2)\mu_{5a}^{(k)}) \sin(kt) \right], \\ \sigma^2 P_1 \kappa_{11} \sum_{k=1}^{\infty} & \left[ (k\eta_{2a}^{(k)} + (kS_1 - g/\sigma^2)\eta_{4a}^{(k)}) \cos(kt) \right. \\ & \left. + (k\mu_{2a}^{(k)} + (kS_1 - g/\sigma^2)\mu_{4a}^{(k)}) \sin(kt) \right]. \end{aligned} \quad (22)$$

Because of (9), neglecting the higher-order terms,  $o(\epsilon)$ , allows for replacing  $g/\sigma^2 \rightarrow g/\sigma_{11}^2$  and, therefore, amplitudes of the first Fourier harmonics are

$$\begin{aligned} \epsilon_x &= P_1 \kappa_{11} (\eta_{1a}^{(1)} - [S_1 - g/\sigma_{11}^2] \eta_{5a}^{(1)}), \quad \bar{\epsilon}_x = P_1 \kappa_{11} (\mu_{1a}^{(1)} - [S_1 - g/\sigma_{11}^2] \mu_{5a}^{(1)}), \\ \bar{\epsilon}_y &= P_1 \kappa_{11} (\eta_{2a}^{(1)} + [S_1 - g/\sigma_{11}^2] \eta_{4a}^{(1)}), \quad \epsilon_y = P_1 \kappa_{11} (\mu_{2a}^{(1)} + [S_1 - g/\sigma_{11}^2] \mu_{4a}^{(1)}). \end{aligned} \quad (23)$$

Here,  $\epsilon_x$  and  $\bar{\epsilon}_x$  appear in the front of  $\cos t$  and  $\sin t$  and imply the forcing components in the  $Ox$  direction, but  $\bar{\epsilon}_y$  and  $\epsilon_y$  correspond to the  $\cos t$  and  $\sin t$  forcing harmonic along the  $Oy$  axis.

Because the first harmonic is not zero (see, (15)), one can assume that  $\epsilon_x^2 + \bar{\epsilon}_x^2 \neq 0$  and, introducing a phase-lag for the input time,

$$\epsilon_x > 0, \quad \bar{\epsilon}_x = 0. \quad (24)$$

This means that the resonant forcing is the same as if the tank performs

the *artificial horizontal harmonic* motions

$$(\kappa_{11}P_1)\eta_1(t) = \epsilon_x \cos t; (\kappa_{11}P_1)\eta_2(t) = \bar{\epsilon}_y \cos t + \epsilon_y \sin t; \eta_4(t) = \eta_5(t) = 0 \quad (25)$$

along the elliptic trajectory

$$\frac{\epsilon_y^2 + \bar{\epsilon}_y^2}{\epsilon_x^2} x^2 + y^2 - 2\frac{\bar{\epsilon}_y}{\epsilon_x} xy = \epsilon_y^2. \quad (26)$$

Without loss of generality, one can assume that the elliptic forcing occurs counterclockwise and, by rotating the  $Oxy$  plane around the  $Oz$  axis leads to a canonic form of (26) so that

$$\epsilon_x > 0, \quad \epsilon_y \geq 0, \quad \bar{\epsilon}_y = \bar{\epsilon}_x = 0. \quad (27)$$

Henceforth, we assume that (27) is satisfied in the appropriate coordinate system with the corresponding phase-lag for the input forcing signal.

To find an asymptotic steady-state solution of the modal system for the elliptic type excitations by (27), we follow the Bubnov–Galerking procedure in [3] by posing the lowest-order components of the primary excited modes as

$$p_{11}(t) = a \cos t + \bar{a} \sin t + O(\epsilon), \quad r_{11}(t) = \bar{b} \cos t + b \sin t + O(\epsilon), \quad (28)$$

where  $a, \bar{a}, \bar{b}$ , and  $b$  are of  $O(\epsilon^{1/3})$ . The corresponding lowest-order free-surface elevations by (28) are a superposition of the two out-of-phase angular modes

$$\zeta(r, \theta, t) = \mathcal{R}_{11}(r)[(a \cos \theta + \bar{b} \sin \theta) \cos t + (\bar{a} \cos \theta + b \sin \theta) \sin t] + o(\epsilon^{2/3}). \quad (29)$$

This implies a swirling wave unless  $(a \cos \theta + \bar{b} \sin \theta)$  and  $(\bar{a} \cos \theta + b \sin \theta)$  define congruent patterns, which happens if and only if

$$ab = \bar{a}\bar{b}. \quad (30)$$

The condition (30) means that (29) determines a *standing* wave.

The second- and third-order generalised coordinates can be found from (11) and (12), (13), respectively. They are

$$p_{0k}(t) = s_{0k}(a^2 + \bar{a}^2 + b^2 + \bar{b}^2)$$

$$+ s_{1k} [(a^2 - \bar{a}^2 - b^2 + \bar{b}^2) \cos 2t + 2(a\bar{a} + b\bar{b}) \sin 2t] + o(\epsilon), \quad (31a)$$

$$p_{2k}(t) = c_{0k}(a^2 + \bar{a}^2 - b^2 - \bar{b}^2) + c_{1k} [(a^2 - \bar{a}^2 + b^2 - \bar{b}^2) \cos 2t + 2(a\bar{a} - b\bar{b}) \sin 2t] + o(\epsilon), \quad (31b)$$

$$r_{2k}(t) = 2c_{0k}(a\bar{b} + b\bar{a}) + 2c_{1k} [(a\bar{b} - b\bar{a}) \cos 2t + (ab + \bar{a}\bar{b}) \sin 2t] + o(\epsilon), \quad (31c)$$

where

$$s_{0k} = \frac{1}{2} \left( \frac{d_{10,k} - d_{8,k}}{\bar{\sigma}_{0k}^2} \right), \quad s_{1k} = \frac{d_{10,k} + d_{8,k}}{2(\bar{\sigma}_{0k}^2 - 4)}, \quad (32)$$

$$c_{0k} = \frac{1}{2} \left( \frac{d_{9,k} - d_{7,k}}{\bar{\sigma}_{2k}^2} \right), \quad c_{1k} = \frac{d_{9,k} + d_{7,k}}{2(\bar{\sigma}_{2k}^2 - 4)}.$$

Substituting (28) and (31) into (10) and gathering the first harmonic terms,  $\cos t$  and  $\sin t$ , lead to the solvability (secular) equations

$$\begin{cases} \textcircled{1}: a [(\bar{\sigma}_{11}^2 - 1) + m_1(a^2 + \bar{a}^2 + \bar{b}^2) + m_3b^2] + \bar{a}[(m_1 - m_3)\bar{b}b + \xi] = \epsilon_x, \\ \textcircled{2}: \bar{a} [(\bar{\sigma}_{11}^2 - 1) + m_1(a^2 + \bar{a}^2 + b^2) + m_3\bar{b}^2] + a[(m_1 - m_3)\bar{b}b - \xi] = 0, \\ \textcircled{3}: b [(\bar{\sigma}_{11}^2 - 1) + m_1(b^2 + \bar{b}^2 + \bar{a}^2) + m_3a^2] + \bar{b}[(m_1 - m_3)\bar{a}a - \xi] = \epsilon_y, \\ \textcircled{4}: \bar{b} [(\bar{\sigma}_{11}^2 - 1) + m_1(b^2 + \bar{b}^2 + a^2) + m_3\bar{a}^2] + b[(m_1 - m_3)\bar{a}a + \xi] = 0 \end{cases} \quad (33)$$

with respect to  $a, \bar{a}, \bar{b}$  and  $b$ ; here,  $\xi = 2\xi_{11}$ , where coefficients  $m_1$  and  $m_3$  are computed by the formulas

$$m_1 = -\frac{1}{2}d_1 + \sum_{j=1}^{I_r} \left[ c_{1j} \left( \frac{1}{2}d_3^{(j)} - 2d_4^{(j)} \right) + s_{1j} \left( \frac{1}{2}d_5^{(j)} - 2d_6^{(j)} \right) - s_{0j}d_5^{(j)} - c_{0j}d_3^{(j)} \right], \quad (34a)$$

$$m_3 = \frac{1}{2}d_1 - 2d_2 + \sum_{j=1}^{I_r} \left[ c_{1j} \left( \frac{3}{2}d_3^{(j)} - 6d_4^{(j)} \right) + s_{1j} \left( -\frac{1}{2}d_5^{(j)} + 2d_6^{(j)} \right) - s_{0j}d_5^{(j)} + c_{0j}d_3^{(j)} \right]. \quad (34b)$$

Coefficients  $m_1$  and  $m_3$  are functions of  $h/r_0$  and the forcing frequency  $\bar{\sigma}_{11}$ . Utilising (9) shows that the latter dependence can be neglected by substituting  $\sigma = \sigma_{11}$  into the corresponding expressions. Dependence on  $\sigma$  remains only in the  $(\bar{\sigma}_{11}^2 - 1)$ -quantity of (33).

After finding  $a, \bar{a}, \bar{b}$  and  $b$  from (33), we can easily compute the second- and third-order components of the asymptotic solution. The second-order quantities are associated with (31), namely, are fully determined by  $a, \bar{a}, \bar{b}$  and  $b$ , but the third-order components are affected by the higher harmonics in (22) as well as the lowest harmonics in the right-hand side of (13).

The linear Lyapunov method and the multitiming technique can be employed to study stability of the constructed asymptotic steady-state solution. This suggests introducing the slowly varying time  $\tau = \frac{1}{2}\epsilon^{2/3}t$  and expressing the perturbed solutions as

$$\begin{aligned} a_1 &= (a + \alpha(\tau)) \cos t + (\bar{a} + \bar{\alpha}(\tau)) \sin t + o(\epsilon^{1/3}), \\ b_1 &= (\bar{b} + \bar{\beta}(\tau)) \cos t + (b + \beta(\tau)) \sin t + o(\epsilon^{1/3}), \end{aligned} \quad (35)$$

where  $a, \bar{a}, b$  and  $\bar{b}$  come from (33). Inserting (35) into the modal equations, gathering terms of the lowest asymptotic quantities order and keeping linear terms in  $\alpha, \bar{\alpha}, \beta$  and  $\bar{\beta}$  lead to the following linear system of ordinary differential equations

$$\mathbf{s}' + \xi \mathbf{s} + \mathcal{S} \mathbf{s} = 0, \quad (36)$$

where  $\mathbf{s} = (\alpha, \bar{\alpha}, \beta, \bar{\beta})^T$ , the prime is the differentiation by  $\tau$ , and the matrix  $\mathcal{S}$  has the following elements

$$\begin{aligned} s_{11} &= -2m_1 a \bar{a} - (m_1 - m_3) b \bar{b}; & s_{13} &= -2m_1 \bar{a} b - (m_1 - m_3) a \bar{b}, \\ s_{12} &= -(\bar{\sigma}_{11}^2 - 1) - m_1(a^2 + 3\bar{a}^2 + b^2) - m_3 \bar{b}^2; & s_{14} &= -2m_3 \bar{a} \bar{b} - (m_1 - m_3) a b, \\ s_{21} &= (\bar{\sigma}_{11}^2 - 1) + m_1(3a^2 + \bar{a}^2 + \bar{b}^2) + m_3 b^2; & s_{22} &= 2m_1 a \bar{a} + (m_1 - m_3) b \bar{b}, \\ s_{23} &= 2m_3 a b + (m_1 - m_3) \bar{a} \bar{b}; & s_{24} &= 2m_1 a \bar{b} + (m_1 - m_3) \bar{a} b, \\ s_{31} &= 2m_1 a \bar{b} + (m_1 - m_3) b \bar{a}; & s_{32} &= 2m_3 \bar{a} \bar{b} + (m_1 - m_3) a b, \\ s_{33} &= 2m_1 b \bar{b} + (m_1 - m_3) a \bar{a}; & s_{34} &= (\bar{\sigma}_{11}^2 - 1) + m_1(b^2 + 3\bar{b}^2 + a^2) + m_3 \bar{a}^2, \\ s_{41} &= -2m_3 a b - (m_1 - m_3) \bar{a} \bar{b}; & s_{42} &= -2m_1 \bar{a} b - (m_1 - m_3) a \bar{b}, \\ s_{43} &= -(\bar{\sigma}_{11}^2 - 1) - m_1(3b^2 + \bar{b}^2 + \bar{a}^2) - m_3 a^2; & s_{44} &= -2m_1 b \bar{b} - (m_1 - m_3) a \bar{a}. \end{aligned}$$

The fundamental solution  $\mathbf{s} = \exp(\lambda\tau)\mathbf{a}$  of (36) follows from the spectral matrix problem  $[(\lambda + \xi)E + \mathcal{S}]\mathbf{a} = 0$ , where  $\lambda$  are the unknown eigenvalues and  $\mathbf{a}$  are the corresponding eigenvectors. Computations give the following characteristic biquadratic equation

$$(\lambda + \xi)^4 + s_1(\lambda + \xi)^2 + s_0 = 0, \quad (37)$$

where  $s_0$  is the determinant of  $\mathcal{S}$  and  $s_1$  is a complicated function of the elements of  $\mathcal{S}$ . The eigenvalues  $\lambda$  can be expressed as  $-\xi \pm \sqrt{x_{1,2}}$ , where  $x_{1,2} = \frac{1}{2}(-s_1 \pm \sqrt{s_1^2 - 4s_0})$  are two solutions of the quadratic equation  $x^2 + s_1x + s_0 = 0$ . The fixed-point solution (associated with  $a, \bar{a}, b$  and  $\bar{b}$ ) is asymptotically stable ( $\alpha, \bar{\alpha}, \beta$  and  $\bar{\beta}$  exponentially decay with  $\tau$ ) if and only if the real component of  $\lambda$  is strongly negative.

In the limit case  $\xi \rightarrow 0$ , the stability condition ( $\Re[\lambda] < 0$ ) takes the following form

$$s_1^2 - 4s_0 \geq 0 \quad \& \quad s_0 \geq 0 \quad \& \quad s_1 \geq 0. \quad (38)$$

For  $O(\epsilon^{2/3}) = \xi > 0$ , the stability condition can be written as the alternative

$$\begin{aligned} &\text{either } s_1^2 - 4s_0 \geq 0 \quad \& \quad -s_1 + \sqrt{s_1^2 - 4s_0} \leq 0 \quad (\Leftrightarrow s_0 \geq 0 \quad \& \quad s_1 \geq 0), \\ &\text{or } s_1^2 - 4s_0 \geq 0 \quad \& \quad -s_1 + \sqrt{s_1^2 - 4s_0} > 0 \quad \& \quad \sqrt{\frac{1}{2} \left( -s_1 + \sqrt{s_1^2 - 4s_0} \right)} < \xi, \\ &\text{or } s_1^2 - 4s_0 < 0 \quad \& \quad \sqrt{2\sqrt{s_0} - s_1} < \xi. \end{aligned} \quad (39)$$

The procedure of finding an analytical solution of the secular system (33) with  $\xi = 0$  (damping is neglected) is in some detail described in [3]. The procedure cannot be generalised to the studied damped sloshing case with  $\xi = O(\epsilon^{2/3})$ . A reason is that the damping causes the two phase-lags,  $\psi$  and  $\varphi$ , for the two lowest (perpendicular, along the  $Ox$  and  $Oy$  directions) modes and, as a consequence, normally, all four amplitude parameters  $a, \bar{a}$  and  $b, \bar{b}$ , are not zero, in the contrast to [3], where the authors proved that  $\bar{a} = \bar{b} = 0$  for longitudinal and elliptic forcing types. A physically-relevant form of (33) should therefore couple the ‘integral’ lowest-order amplitudes  $A, B$  and the phase-lags  $\psi, \varphi$ :

$$A = \sqrt{a^2 + \bar{a}^2} \quad \text{and} \quad B = \sqrt{\bar{b}^2 + b^2} > 0, \quad (40a)$$

$$a = A \cos \psi, \quad \bar{a} = A \sin \psi, \quad \bar{b} = B \cos \varphi, \quad b = B \sin \varphi. \quad (40b)$$

Inserting (40) into expressions  $\bar{a}$  ① –  $a$  ②,  $\bar{b}$  ③ –  $b$  ④,  $a$  ① +  $\bar{a}$  ② and  $b$  ③ +  $\bar{b}$  ④ of (33) derives the following alternative secular equations

$$\begin{cases} \boxed{1} : A[\Lambda + m_1 A^2 + (m_3 - \mathcal{F})B^2] = \epsilon_x \cos \psi, & \boxed{3} : A[\mathcal{D}B^2 + \xi] = \epsilon_x \sin \psi, \\ \boxed{2} : B[\Lambda + m_1 B^2 + (m_3 - \mathcal{F})A^2] = \epsilon_y \sin \varphi, & \boxed{4} : B[\mathcal{D}A^2 - \xi] = \epsilon_y \cos \varphi, \end{cases} \quad (41a)$$

$$\begin{aligned}\mathcal{F} &= (m_3 - m_1) \cos^2(\alpha) = (m_3 - m_1)/(1 + C^2), \\ \mathcal{D} &= (m_3 - m_1) \sin(\alpha) \cos(\alpha) = (m_3 - m_1)C/(1 + C^2),\end{aligned}\quad (41b)$$

where

$$\Lambda = \bar{\sigma}_{11}^2 - 1, \quad \alpha = \varphi - \psi, \quad C = \tan \alpha, \quad 0 \leq \epsilon_y \leq \epsilon_x \neq 0,$$

( $\mathcal{F}(\alpha)$  and  $\mathcal{D}(\alpha)$  are the  $\pi$ -periodic functions of the phase-lags difference  $\alpha$ ). The secular systems (33) and (41) are *mathematically equivalent*, i.e., getting known  $A, B, \psi, \varphi$  from (41) computes  $a, \bar{a}, b, \bar{b}$  and *vice versa*.

In terms of definitions (40) and (41), the standing wave condition (30) is equivalent to

$$\sin \alpha = 0 \quad \Leftrightarrow \quad C = 0 \quad (42)$$

so that the non-zero  $C$  implies swirling.

## 5 Response curves in the $(\sigma/\sigma_{11}, A, B)$ space

**Longitudinal forcing.** Undamped resonant steady-state sloshing due to longitudinal excitations ( $\epsilon_y = 0, \xi = 0$ ) was analysed in [3] to prove that  $\bar{a} = \bar{b} = 0$  is fulfilled for any admissible input parameters and there exist two physically-different solutions of (33) corresponding to the so-called *planar* standing wave ( $b = 0$  and (30) is satisfied) and *swirling* ( $ab \neq 0$  in (30)). In terms of the secular equations (40) and (41) with  $\xi = 0$ , these two steady-state solutions imply  $B = 0, \sin \psi = 0, C = 0$  and  $AB \neq 0, \sin \psi = \cos \varphi = 0$  ( $C = \pm\infty$ ), respectively. In addition, one should remember that swirling consists of two identical angular progressive waves occurring in counter- and clockwise directions, these two waves correspond to  $C = +\infty$  and  $-\infty$ , respectively.

For the non-zero damping  $\xi \neq 0$  and  $\epsilon_y = 0$  (damped steady-state sloshing due to longitudinal excitations), the secular system (41) has the same two physically-different solutions implying *planar* sloshing with the zero transverse amplitude  $B = 0$  but  $A, \psi$  are computed by  $\boxed{1}^2 + \boxed{3}^2 =$

$$= A^2 [(\Lambda + m_1 A^2)^2 + \xi^2] = \epsilon_x^2; \quad 0 < A \leq \frac{\epsilon_x}{\xi}; \quad \psi = \arccos \frac{A(A + m_1 A^2)}{\epsilon_x}, \quad (43)$$

and *swirling* with  $B \neq 0$ , which can be computed by rewriting (41) in

the form

$$\begin{cases} A \left[ \Lambda + m_1 A^2 + \frac{m_1 + m_3 C^2}{1 + C^2} B^2 \right] = \epsilon_x \cos \psi; \\ A \left[ \frac{(m_3 - m_1)C}{1 + C^2} B^2 + \xi \right] = \epsilon_x \sin \psi; \\ B^2 = -\frac{1}{m_1} \left[ \Lambda + \frac{m_1 + m_3 C^2}{1 + C^2} A^2 \right] > 0; A^2 = \frac{\xi(1 + C^2)}{(m_3 - m_1)C} > 0. \end{cases} \quad (44)$$

Consequently substituting expressions for  $A^2$  and  $B^2$  of (44) into the square sum of the first row equations, derives the cubic equation with respect to  $C$ :

$$P_l(C) = q_3 C^3 + q_2 C^2 + q_1 C + q_0 = 0, \quad (45)$$

where

$$\begin{aligned} q_3 &= \xi^3 (m_1 + m_3)^2 > 0, & q_2 &= 2\xi^2 \Lambda (m_3^2 - m_1^2), \\ q_1 &= \xi [4\xi^2 m_1^2 + \Lambda^2 (m_1 - m_3)^2], & q_0 &= \epsilon_x^2 m_1^2 (m_1 - m_3). \end{aligned}$$

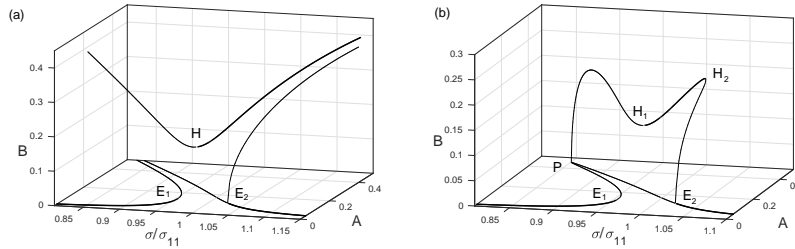


**Figure 3.** Response curves in the  $(\sigma/\sigma_{11}, A, B)$ -space for the longitudinal harmonic forcing in the  $Oxz$ -plane,  $h/r_0 = 1.5$ , the nondimensional forcing amplitude  $\eta_{1a} = 0.01$  ( $\eta_{2a} = 0$ ). The branches are computed by using (43) for planar ( $B = 0$ ) and (44) is used for swirling ( $B > 0$ ) wave regimes. The bold lines mark stable solutions. The undamped sloshing ( $\xi = 0$ ) is presented in (a) and the damped one ( $\xi = 0.02$ ) is shown in (b). There are no stable steady-state sloshing between  $E_1$  and  $E_2$  where irregular (chaotic) waves are expected. Curves on the  $(\sigma/\sigma_{11}, A)$  plane correspond to the planar wave regime. The damping causes the response curves do not go to infinity. An extra bifurcation point  $P$  exists where swirling emerges from the planar wave branching.

Illustrative response curves for undamped (a) and damped (b) steady-state sloshing are shown in figure 3. The computations were made with  $h/r_0 = 1.5$ , the forcing amplitude is  $\eta_{1a} = 0.01$ , and the damping coefficients  $\xi = 2\xi_{11} = 0.02$  (in (b)). The response curves for undamped sloshing in (a) were discussed in [3, 4, 10]. For this case, we see the branches belonging to the plane  $(\sigma/\sigma_{11}, A)$  responsible for planar wave regime. The stable planar sloshing is located to the left of  $E_1$  and to the right of  $E_2$ . The planar sloshing waves become unstable in a neighbourhood of the primary resonance  $\sigma/\sigma_{11} = 1$  where stable swirling (to the right of  $H$ ) and irregular waves (there are no stable steady-state sloshing) between  $E_1$  and  $H$  are predicted. The non-zero damping removes infinite points as shown in (b). However, stability ranges of planar and swirling waves are weakly affected by  $\xi = 0.02$  so that positions of  $E_1, E_2$  and  $H_1$  (replaces  $H$ ) determining these ranges are almost the same. A novelty is two points  $H_2$  and  $P$ , which can be treated as bifurcation points where swirling emerges from the planar steady-state sloshing. The steady-state swirling branching constitutes an arc, which is pinned at these two points.

As mentioned in [3], the undamped steady-state sloshing is characterised by piece-wise values of the phase lags  $\psi$  and  $\varphi$ :  $\sin \psi = 0$  for the planar wave regime and  $\sin \psi = \cos \varphi = 0$  for swirling. The damping makes the phase lags by amplitude (frequency) dependent functions keeping  $C = \tan(\varphi - \psi) \geq 0$ . For the planar wave regime by (42),  $\varphi = \psi \pm \pi$ , but swirling causes finite and positive  $C > 0$ ,  $C \neq +\infty$ . The latter inequality follows from the last expression of (44), in which  $m_3 > m_1$ . The positive numbers  $C = \tan \alpha > 0$  are the roots of (45). The phase lag  $\psi$  comes from the first two equations of (42) for any given point on the  $(\sigma/\sigma_{11}, A, B)$  curves. For each  $\psi$  of the swirling wave regime, there are two different phase lags  $\varphi_1 = \psi + \alpha$  and  $\varphi_2 = \psi + \alpha \pm \pi$ . Physically, these two phase lags  $\varphi_{1,2}$  for each point on the arc  $P, H_1, H_2, E_2$  mean that two physically-identical swirling waves (clockwise and counterclockwise) are possible.

**Elliptic forcing** ( $\epsilon_y = \delta\epsilon_x$ ,  $0 < \delta < 1$ ). The *undamped sloshing* with  $\xi = 0$  in [3] was characterised by  $\bar{a} = \bar{b} = 0$ . Indeed, using [3] and [4] as well as taking  $\bar{b}$  ① –  $a$  ④ and  $\bar{a}$  ③ –  $b$  ④ make it possible to derive the linear algebraic system

$$\bar{a} - \delta\bar{b} = \xi(A^2 + B^2)/\epsilon_x, \quad \delta\bar{a} - \bar{b} = \xi(m_1 - m_3)(AB/\epsilon_x) \sin \alpha, \quad (46)$$

with respect to  $\bar{a}$  and  $\bar{b}$  whose determinant is equal to  $\delta^2 - 1$ . Obviously, (46) has only trivial solution  $\bar{a} = \bar{b} = 0$  as  $\xi = 0$  and  $0 \leq \delta < 1$ .

As a consequence, the undamped elliptically-forced sloshing turns  $\boxed{3}$  and  $\boxed{4}$  into identities, but the phase lags  $\psi$  and  $\varphi$  satisfy the condition  $\sin \psi = \cos \varphi = 0$  and, therefore,  $\cos \alpha = 0$  and  $\sin \alpha = \pm 1$ . The amplitudes  $A = |a|$  and  $B = |b|$  and, therefore, the remaining two equations  $\boxed{1}$  and  $\boxed{2}$  read as

$$A^2[\Lambda + m_1 A^2 + m_3 B^2] = \epsilon_x^2, \quad B^2[\Lambda + m_1 B^2 + m_3 A^2] = \delta^2 \epsilon_x^2. \quad (47)$$

This system with respect to  $A^2$  and  $B^2$  can be analytically solved as described in [3].

The present paper focuses on the *damped* sloshing with  $\xi \neq 0$  in (41a). Obviously, the system (46) has then no trivial solution. The phase lags  $\varphi$  and  $\psi$  are rather complicated functions of the input parameters. Both the amplitudes  $A$ ,  $B$  and the phase lags  $\varphi$ ,  $\psi$  should be found from the nonlinear system (41a).

Let us exclude  $\varphi$  and  $\psi$  and reduce (41a) to a system of three equations with respect  $A$ ,  $B$  and  $C$ . For this purpose, we insert  $\varphi = \psi + \alpha$  into the right-hand sides of  $\boxed{2}$  and  $\boxed{4}$  and substitute  $\epsilon_x \cos \psi$  and  $\epsilon \sin \psi$  taken from  $\boxed{1}$  and  $\boxed{3}$ . The result is the following linear system of homogeneous equations

$$\begin{cases} (\delta A)[\cos \alpha(\mathcal{D}(C)B^2 + \xi) + \sin \alpha(\Lambda + m_1 A^2 + (m_3 - \mathcal{F}(C))B^2)] \\ \quad - B[\Lambda + m_1 B^2 + (m_3 - \mathcal{F}(C))A^2] = 0, \\ (\delta A)[\cos \alpha(\Lambda + m_1 A^2 + (m_3 - \mathcal{F}(C))B^2) - \sin \alpha(\mathcal{D}(C)B^2 + \xi)] \\ \quad - B[\mathcal{D}(C)A^2 - \xi] = 0, \end{cases}$$

with respect to  $\delta A$  and  $B$ . The system must have a nontrivial solution. This leads to the zero-determinant condition

$$\xi(A^2 - B^2)\mathcal{D}(C) - \mathcal{F}(C)[\xi^2 + (\Lambda + m_1(A^2 + B^2))^2]/(m_3 - m_1) + A^2 B^2 \mathcal{D}^2(C) = 0, \quad (48)$$

which couples  $A^2$ ,  $B^2$  and  $C$ . Another two equations with respect to  $A^2$ ,  $B^2$  and  $C$  come from  $\boxed{1}^2 + \boxed{3}^2$  and  $\boxed{2}^2 + \boxed{4}^2$  and take the form

$$\begin{cases} A^2[(\Lambda + m_1 A^2 + (m_3 - \mathcal{F})B^2)^2 + (\mathcal{D}B^2 + \xi)^2] = \epsilon_x^2, \\ B^2[(\Lambda + m_1 B^2 + (m_3 - \mathcal{F})A^2)^2 + (\mathcal{D}A^2 - \xi)^2] = \delta^2 \epsilon_x^2. \end{cases} \quad (49)$$

The system (48), (49) is a base for getting the response curves in the  $(\sigma/\sigma_{11}, A, B)$  space. One can prove that  $C \neq 0$  since  $C = 0$  leads to (48)

$\Rightarrow \xi^2 + (\Lambda + m_1(A^2 + B^2))^2 = 0$  and (49)  $\Rightarrow A^2[\xi^2 + (\Lambda + m_1(A^2 + B^2))^2] = \epsilon_x^2 \neq 0$ , simultaneously. Physically,  $C \neq 0$  means that *there are no standing wave regimes* for the elliptic forcing. All steady-state sloshing regimes are *swirling*. Our numerical experiments show that  $C > 0$  as  $(m_3 - m_1) > 0$ .

The authors do not know how to get an analytical solution of (48), (49). A numerical scheme is used. We define  $\mathcal{F}$  and  $\mathcal{D}$  as functions of  $0 < \beta < 1$

$$\mathcal{F}(\beta) = (m_3 - m_1)\beta, \quad \mathcal{D}(\beta) = (m_3 - m_1) \operatorname{sgn}(C) \sqrt{\beta(1 - \beta)}. \quad (50)$$

When  $C > 0$ , a simple analysis shows that

$$0 < A < \frac{\epsilon_x}{\xi}, \quad 0 < B^2 \leq \min \left[ \frac{1}{\mathcal{D}(\beta)} \left( \frac{\epsilon_x}{A} - \xi \right), \frac{\delta^2 \epsilon_x^2}{(\mathcal{D}(\beta)A^2 - \xi)^2} \right], \quad (51)$$

which determines the fixed interval for  $A$  but the interval for  $B^2$  is determined by  $A$  and  $\beta$ . The first equation of (49) computes the two real  $\Lambda_{1,2}$  for any given  $0 < \beta < 1$  and  $A, B^2$  satisfying (51) as follows

$$\Lambda_{1,2} = -m_1 A^2 - (m_3 - \mathcal{F}(\beta))B^2 \pm \sqrt{\frac{\epsilon_x^2}{A^2} - (\mathcal{D}(\beta)B^2 + \xi)^2}. \quad (52)$$

Furthermore, to solve (48), (49) for *any fixed*  $A$  belonging to the corresponding interval of (51)

- 1) we introduce a mesh  $0 < \beta_1 < \beta_2 < \dots < \beta_k < \dots < \beta_K < 1$ ;
- 2) for any fixed  $\beta_k \in \{\beta_n\}$ , we solve the two equations (follow from the second equation of (49))

$$[\Lambda_j + m_1 B^2 + (m_3 - \mathcal{F}(\beta))A^2]^2 + [\mathcal{D}(\beta)A^2 - \xi]^2 = \frac{\delta^2 \epsilon_x^2}{B^2}, \quad j = 1, 2, \quad (53)$$

(associated with  $+$  and  $-$  in expression (52)) with respect to  $B^2$  on the interval by (51); the result is a set of positive roots  $B_{k,j,i}^2 = B_i^2(A, \beta_k, j)$ ,  $j = 1, 2$ , for each  $A$  and  $\beta_k$ ;

- 3) each root  $B_i(A, \beta_k, j)$  is subsequently substituted into (48):

$$\xi(A^2 - B_{i,k,j}^2) \mathcal{D}(\beta_k) - \mathcal{F}(\beta_k) [\xi^2 + (\Lambda_j + m_1(A^2 + B_{i,k,j}^2))^2] / (m_3 - m_1)$$

$$+ A^2 B_{i,k,j}^2 \mathcal{D}^2(\beta_k) = 0 \quad (54)$$

to detect the mesh interval  $(\beta_k, \beta_{k+1})$ , where the left-hand side of (54) changes the sign;

- 4) an iterative procedure is used to compute  $\beta \in (\beta_k, \beta_{k+1})$  and the corresponding  $B_i(A, \beta, j)$ .

The algorithm computes the solution for any fixed  $A$ . Varying  $A$  in the interval by (51) outputs response curves in the  $(\sigma/\sigma_{11}, A, B)$  space, which are presented in figures 4-7.

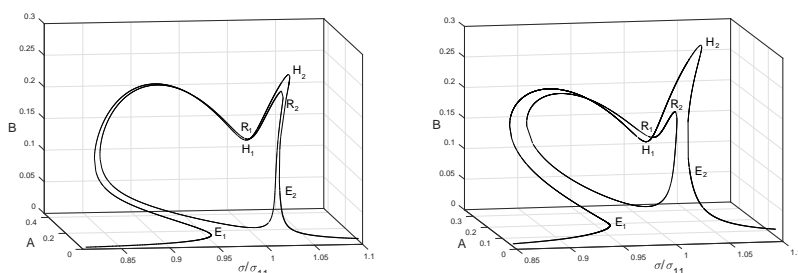


**Figure 4.** Response curves in the  $(\sigma/\sigma_{11}, A, B)$ -space for the steady-state resonant sloshing due to an elliptic counterclockwise forcing with  $\eta_{1a} = 0.01$ ,  $\eta_{2a} = \delta\eta_{1a}$ ;  $\delta = 0.05$  in the left panel and  $0.2$  in the right one;  $\xi = 0.02$ . All response curves correspond to swirling but some subbranches are close to the  $(\sigma/\sigma_{11}, A)$ -plane that means that sloshing is of an almost standing (planar) wave type. The branch containing  $E_1, H_1, H_2, E_2$  implies swirling, which co-directed with the elliptic forcing but the loop-like branch with  $R_1$  and  $R_2$  marks the counter-directed swirling. The bold lines imply stability.

Figure 4 shows that, by introducing a non-zero positive  $\delta$  implying an elliptic counterclockwise forcing with a small semi-axis along  $Oy$  splits the arc  $PH_1H_2E_2$  in figure 3 (b), whose points determine two identical co- and counterclockwise swirling waves, into two different branches. The first branch contains points  $E_1, H_1, H_2, E_2$ ; it exists far from the primary resonance zone, where the co-directed stable swirling wave is close to a standing planar wave. The corresponding subbranches are to the left of  $E_1$  and to the right of  $E_2$ . Another stability subbranch is the piece  $H_1H_2$ . The second loop-like branch with  $R_1$  and  $R_2$  implies swirling, which is counter-directed to the forcing. This swirling is stable on  $R_1R_2$ .

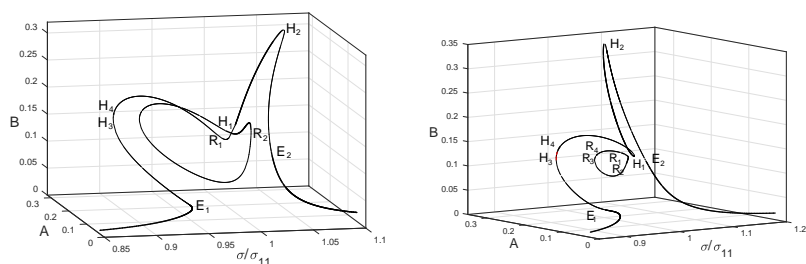


**Figure 5.** The same as in figure 4 but for  $\delta = 0.3$  (the left panel) and  $0.45$  (the right one). An extra range of the co-directed (with respect to the forcing) swirling  $H_3H_4$  appears with increasing  $\delta$  but the stable counter-directed swirling (points  $R_1R_2, R_3R_4$ ) vanishes with increasing  $\delta$ .

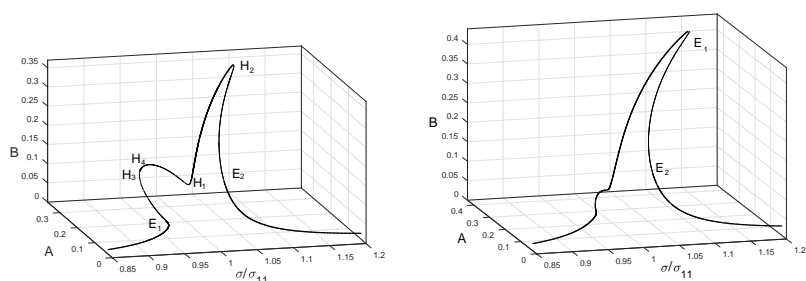


**Figure 6.** The same as in figure 4 but for  $\delta = 0.5$  (the left panel) and  $0.8$  (the right one). In contrast to the undamped case in [3], there are no counter-directed swirling at all.

There is the frequency range between  $E_1$  and  $H_1$  where the theory does not predict stable steady-state sloshing and irregular (chaotic) waves are expected.

Increasing the semi-axes ratio  $\delta$  decreases the loop-like  $R$  branch responsible for the counter-directed swirling. Figure 5 demonstrates this fact for  $\delta = 0.3$  and  $0.45$ . Decreasing the  $R$ -branch means that the linear damping makes the counter-directed swirling impossible when passing from longitudinal to rotary forcing types. In the contrast, the theoretical undamped analysis in [3] shows that the counter-directed propagating wave exists and may be stable in a frequency range for any  $0 < \delta < 1$ .

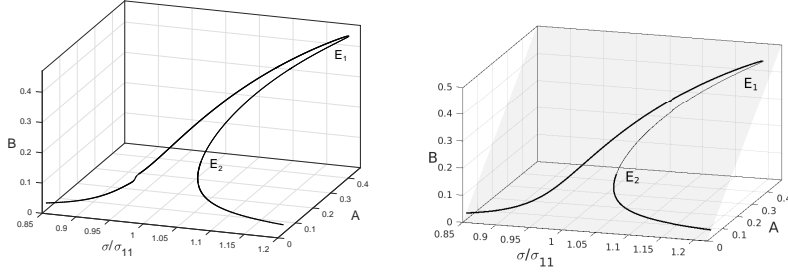


**Figure 7.** The same as in figure 6 but for an almost rotary forcing with  $\delta = 0.95$  (the left panel) and rotary excitations with  $\delta = 1.0$  (the right panel).

The non-zero  $\xi$  leads to vanishing the  $R$  branch as  $\delta$  increases. When  $\xi = 0.02$ , this happens for  $\delta$  slightly lower than 0.5. As a consequence, we do not see this branch in figure 6, where  $\delta = 0.5$  and 0.8.

In figures 5 and 6, we also see extra islands of stability  $H_3H_4$  and  $R_3R_4$ . After vanishing the  $R$  branch, the island  $H_3H_4$  grows up to connect other stable subbranches.

**Rotary forcing** ( $\epsilon_x = \epsilon_y$ ). The undamped analysis [3] showed that the rotary (orbital circular) forcing causes a non-uniqueness of the steady-state solution, i.e. the secular system becomes degenerated. The paper established wave regimes consisting of a superposition of swirling waves in both directions and a planar standing wave. However, only co-directed swirling has been stable according to [3].

To study the damped sloshing by using the secular system (48), (49) with  $\delta = 1$  and  $\xi \neq 0$ , we recall that  $C \neq 0$  but the limit  $C \rightarrow +\infty$  is possible. This limit implies the co-directed rotary wave. It transforms (48) to  $A^2 = B^2$  and the two equations (49) become equivalent

$$A = B > 0; \quad A^2(\Lambda + (m_1 + m_3)A^2)^2 + \xi^2 = \epsilon_x^2. \quad (55)$$

For the rotary co-directed sloshing,  $\mathcal{D} = \mathcal{F} = 0$ , that makes it possible to restore  $\psi$  and  $\varphi - \psi = \pi/2$ . Numerical experiments show that (48), (49) with  $\xi \neq 0$  has no solution except the analytical solution (55).

Figure 7 illustrates the passage  $\delta \rightarrow 1$  by drawing the response curves with  $\delta = 0.95$  and 1. This hard-spring response is experimentally confirmed in [17].

## 6 Conclusions

The multimodal theory of the steady-state sloshing in an upright circular tank from [3] is generalised by adding the linear damping terms. We show that the linear damping matter for relatively small containers, which could be laboratory tanks, e.g., bioreactors. Because any periodic orbital tank forcing with four degrees of freedom (sway/surge/pitch/roll) are, within to higher order contributions, equivalent to an artificial elliptic horizontal tank excitation, the study concentrates on the steady-state wave regimes occurring due to these elliptic excitations with different semi-axes ratios  $\delta$ .

For the longitudinal forcing, the linear damping leads to extra bifurcation points on the response curves where swirling emerges from the planar wave regime. Each point on the swirling-related branch implies two physically identical but counter-directed progressive angular waves. Non-zero semi-axes ratio splits the branch into two non-connected parts, one of which corresponds to swirling, which is co-directed with the forcing, but another part implies a counter-directed swirling. For smaller ratios, both parts exist and there are frequency ranges where the corresponding steady-state waves are stable. Increasing the semi-axes ratio makes the second branching part (counter-directed swirling) smaller so that it finally vanishes at a certain  $\delta$ . This is opposite to the undamped case [3], when the counter-directed swirling was co-existing for any  $0 < \delta \leq 1$ .

- [1] *Barnyak M. Ya., Leshchuk O. P.* Construction of solutions of the problem of free oscillations of viscous fluid in a half-filled spherical tank // *Nonlinear Oscillations*.— 2008.— **11**, Issue 4.— P. 461–483.
- [2] *Ducci A., Weheliye W. H.* Orbitally shaken bioreactors – viscosity effects on flow characteristics // *AIChE Journal*.— 2014.— **60**.— P. 3951–3968.
- [3] *Faltinsen O. M., Lukovsky I. A., Timokha A. N.* Resonant sloshing in an upright tank // *Journal of Fluid Mechanics*.— 2016.— **804**.— P. 608–645.
- [4] *Faltinsen O. M., Timokha A. N.* *Sloshing*. — Cambridge University Press, 2009. — 686 p.
- [5] *Henderson D. M., Miles J. W.* Surface-wave damping in a circular cylinder with a fixed contact angle // *Journal of Fluid Mechanics*.— 1994.— **275**.— P. 285–299.
- [6] *Ibrahim R. A.* Recent advances in physics of fluid parametric sloshing and related problems // *Journal of Fluids Engineering*.— 2015.— **137**.— Paper ID 090801-1.— P. 1–52.

- 
- [7] *Ikeda T., Ibrahim R. A., Harata Y., Kuriyama T.* Nonlinear liquid sloshing in a square tank subjected to obliquely horizontal excitation // *Journal of Fluid Mechanics.*—2012.—**700.**—P. 304–328.
- [8] *Keulegan G.* Energy dissipation in standing waves in rectangular basins // *Journal of Fluid Mechanics.*—1959.—**6.**—P. 33–50.
- [9] *Kim H. M., Kizito J.* Stirring free surface flows due to horizontal circulatory oscillation of a partially filled container // *Chem. Eng. Comm.*—2009.—**196.**—P. 1300–1321.
- [10] *Lukovsky I. A.* Nonlinear dynamics: mathematical models for rigid bodies with a liquid.—De Gruyter, 2015.—400 p.
- [11] *Lukovsky I., Timokha A.* Combining Narimanov–Moiseev’ and Lukovsky–Miles’ schemes for nonlinear liquid sloshing // *Journal of Numerical and Applied Mathematics.*—2011.—**105.**—P. 69–82.
- [12] *Lukovsky I. A., Timokha A. N.* Multimodal method in sloshing // *Journal of Mathematical Sciences.*—2017.—**220.**—P. 239–253.
- [13] *Martel A., Nicolas J. A., Vega J. M.* Surface-wave damping in a brimful circular cylinder // *Journal of Fluid Mechanics.*—1998.—**360.**—P. 213–228.
- [14] *Miles J. W.* A note on interior vs. boundary-layer damping of surface waves in a circular cylinder // *Journal of Fluid Mechanics.*—1998.—**364.**—P. 319–323.
- [15] *Raynovskyy I., Timokha A.* Resonant liquid sloshing in an upright circular tank performing a periodic motion // *Journal of Numerical and Applied Mathematics.*—**2,** Issue 122.—P. 71–82.
- [16] *Reclari M.* Hydrodynamics of orbital shaken bioreactors.—PhD Thesis No 5759.—Ecole Polytechnique Federale de Lausanne, 2013.—159 pp.
- [17] *Reclari M., Dreyer M., Tissot S., Obreschkow D., Wurm F. M., Farhat M.* Surface wave dynamics in orbital shaken cylindrical containers // *Physics of Fluids.*—2014.—**26.**—Paper No 052104.—P. 1–11.
- [18] *Royon-Lebeaud A., Hopfinger E., Cartellier A.* Liquid sloshing and wave breaking in circular and square-base cylindrical containers // *Journal of Fluid Mechanics.*—2007.—**577.**—P. 467–494.
- [19] *Weheliye W., Yianneskis M., Ducci A.* On the fluid dynamics of shaken bioreactors – flow characterization and transition // *AIChE Journal.*—2013.—**59.**—P. 334–344.